Since January 2020 Elsevier has created a COVID-19 resource centre with free information in English and Mandarin on the novel coronavirus COVID-19. The COVID-19 resource centre is hosted on Elsevier Connect, the company's public news and information website.

Free Radical Biology and Medicine 172 (2021) 688–698

Contents lists available at ScienceDirect

Free Radical Biology and Medicine

journal homepage: www.elsevier.com/locate/freeradbiomed

Upregulation of oxidative stress gene markers during SARS-COV-2 viral infection

Narjes Saheb Sharif-Askari [a], Fatemeh Saheb Sharif-Askari [a], Bushra Mdkhana [a], Hawra Ali Hussain Alsayed [b], Habiba Alsafar [c,d,e,f], Zeyad Faoor Alrais [g], Qutayba Hamid [h,i], Rabih Halwani [h,j,*]

[a] Sharjah Institute of Medical Research, University of Sharjah, Sharjah, United Arab Emirates
[b] Pharmacy Department, Dubai Health Authority, Dubai, United Arab Emirates
[c] Department of Biomedical Engineering, College of Engineering, Khalifa University of Science and Technology, Abu Dhabi, United Arab Emirates
[d] Center for Biotechnology, Khalifa University of Science and Technology, Abu Dhabi, United Arab Emirates
[e] Department of Biomedical Engineering, College of Engineering, Khalifa University of Science and Technology, Abu Dhabi, United Arab Emirates
[f] Department of Genetics and Molecular Biology, College of Medicine and Health Sciences, Khalifa University of Science and Technology, Abu Dhabi, United Arab Emirates
[g] Anaesthesia and Intensive Care Unit, Dubai Health Authority, Dubai, United Arab Emirates
[h] Department of Clinical Sciences, College of Medicine, University of Sharjah, Sharjah, United Arab Emirates
[i] Meakins-Christie Laboratories, Research Institute of the McGill University Healthy Center, McGill University, Montreal, QC, Canada
[j] Prince Abdullah Ben Khaled Celiac Disease Research Chair, Department of Pediatrics, Faculty of Medicine, King Saud University, Saudi Arabia

ARTICLE INFO

Keywords:
SARS-COV-2
COVID-19
Oxidative stress
Antioxidant
Pro-oxidant
Neutrophils
Myeloperoxidase
Calprotectin
S100A8
S100A9
Bioinformatics
Saliva
Lung autopsies
Respiratory viral infection

ABSTRACT

Severe viral infections, including SARS-COV-2, could trigger disruption of the balance between pro-oxidant and antioxidant mediators; the magnitude of which could reflect the severity of infection and lung injury. Using publicly available COVID-19 transcriptomic datasets, we conducted an in-silico analyses to evaluate the expression levels of 125 oxidative stress genes, including 37 pro-oxidant genes, 32 oxidative-responsive genes, and 56 antioxidant genes. Seven oxidative stress genes were found to be upregulated in whole blood and lung autopsies (MPO, S100A8, S100A9, SRXN1, GCLM, SESN2, and TXN); these genes were higher in severe versus non-severe COVID-19 leucocytes. Oxidative genes were upregulated in inflammatory cells comprising macrophages and $CD8^+$ T cells isolated from bronchioalveolar fluid (BALF), and neutrophils isolated from peripheral blood. MPO, S100A8, and S100A9 were top most upregulated oxidative markers within COVID-19's lung autopsies, whole blood, leucocytes, BALF derived macrophages and circulating neutrophils. The calprotectin's, S100A8 and S100A9 were upregulated in SARS-COV-2 infected human lung epithelium. To validate our in-silico analysis, we conducted qRT-PCR to measure MPO and calprotectin's levels in blood and saliva samples. Relative to uninfected donor controls, MPO, S100A8 and S100A9 were significantly higher in blood and saliva of severe versus asymptomatic COVID-19 patients. Compared to other different viral respiratory infections, coronavirus infection showed a prominent upregulation in oxidative stress genes with MPO and calprotectin at the top of the list. In conclusion, SARS-COV-2 induce the expression of oxidative stress genes via both immune as well as lung structural cells. The observed correlation between oxidative stress genes dysregulation and COVID-19 disease severity deserve more attention. Mechanistical studies are required to confirm the correlation between oxidative stress gene dysregulation, COVID-19 severity, and the net oxidative stress balance.

1. Introduction

The severity of coronavirus disease 2019 (COVID-19), caused by severe acute respiratory syndrome coronavirus 2 (SARS-COV-2), ranges from asymptomatic to life-threatening infection [1–4]. Severe COVID-19 disease has been associated with innate immune dysregulation, early immunosuppression, lymphopenia, vascular thrombosis, hypoxia, and cytokine storm [5–8].

Many severe viral infections cause oxidative mediated cellular injury

* Corresponding author. Department of Clinical Sciences, College of Medicine, University of Sharjah, Sharjah, United Arab Emirates
E-mail address: rhalwani@sharjah.ac.ae (R. Halwani).

https://doi.org/10.1016/j.freeradbiomed.2021.06.018
Received 4 May 2021; Received in revised form 3 June 2021; Accepted 21 June 2021
Available online 26 June 2021

through activation of phagocytes, production of reactive oxygen species, and release of pro-oxidant cytokine and inflammatory mediators.

Abbreviations

AMPK	AMP-activated protein kinase
ARDS	Acute respiratory distress syndrome
AREs	Antioxidant response elements
BALF	Bronchioalveolar fluid
COVID-19	Coronavirus disease 2019
DEGs	Differentially expressed genes
DSREC	Dubai Scientific Research Ethics Committee
FC	Fold-change
GO	Gene Ontology
IAV	Influenza A
ICU	Intensive care unit
IQR	Interquartile range
NETs	Neutrophil extracellular traps
NOX2	NAPDH oxidase
NRF2	Nuclear factor-erythroid 2 related factor 2
PBMCs	Peripheral blood mononuclear cells
RMA	Robust Multi-Array Average
RSV	Respiratory syncytial virus
SARS-COV-2	Severe acute respiratory syndrome coronavirus 2
SOD	Superoxide dismutase
TLR4	Toll-like receptor 4

Similarly, SARS-COV-2 respiratory viral infection could trigger disruption of the balance between pro-oxidant and antioxidant mediators; the magnitude of this imbalance could, hence, reflect the severity of COVID-19 disease and lung injury. In fact, comorbidities with known impaired redox balance such as cardiometabolic disorders, cancer, and chronic obstructive pulmonary diseases were associated with severe COVID-19 and high mortality rate [9–11].

Oxidative stress level predicts poor prognosis in respiratory viral infection. NAPDH oxidase (NOX2) and dual oxidase enzymes (Duox1 and Duox2) pro-oxidative markers are induced by influenza A (IAV) infection and cause severe lung injury [12]. In addition, production of neutrophil extracellular traps and myeloperoxidase oxidants are triggered by H7N9 and H1N1 viral infection, and correlate with poor prognosis [13]. Alternatively, severe respiratory syncytial virus bronchiolitis cause decrease in expression of antioxidant markers including Superoxide dismutase (SOD), catalase, and glutathione peroxidase [14].

SARS-COV-2 infect lung cells by binding to the host ACE2 receptors that are abundantly expressed in both type II alveolar epithelial cells [15] and multi-ciliated epithelial cells [16]. This viral infection could potentially cause acute respiratory distress syndrome (ARDS) with extreme drop in ACE2 levels [17,18]. ACE2 plays a critical role in regulation of redox balance; it catalyzes conversion of vasoconstrictor angiotensin II peptide into vasodilator angiotensin1-7. The down-regulation of ACE2 expression observed with SARS-C-OV-2 infection, would enable unopposed binding of angiotensin II to AT1 receptors, which in turn activates NADPH oxidase, and augments production of reactive oxygen species [19,20]. Expected Cellular response to oxidative stress is mediated by Nuclear factor-erythroid 2 related factor 2 (NRF2) which activate the host antioxidant defense by encoding transcription of oxidative-responsive and antioxidant genes which contain antioxidant response elements (AREs) including thioredoxins, sestrins, and glutathione system [21–23]. The protective NRF2 antioxidant signaling was found to be suppressed in severe COVID-19 lung autopsies as well as SARS-COV-2 in-vitro infection model [24]. These findings could suggest that SARS-COV-2 target NRF2 as an evasion mechanism to enhance their viral survival and replication [24].

Although the contribution of oxidative stress to disease pathogenesis had been explored in several viral infection [28,29], its relevance to COVID-19 respiratory infection deserves more attention [25,26]. This is due to the fact that immune derangement during SARS-C-OV-2 infection could switch on a lethal cycle of oxidative stress, inflammation and lung tissue injury. Therefore, the aim of the current study is to evaluate the dysregulation of oxidative balance during SARS-COV-2 infection through measuring the gene expression levels of 125 oxidative stress genes known to be associated with proinflammatory, antimicrobial, oxidant-scavenging and apoptosis-inducing activities.

2. Method

For this study, we first established a list of 125 oxidative stress genes including: 37 pro-oxidant genes, 32 oxidative-responsive genes, and 56 antioxidant genes (Tables 1–3). The oxidative stress genes were derived from Gene Ontology (GO) term: 0006979 (response to oxidative stress), WikiPathways oxidative stress database [27], and a number of previous reports [28–31]. The expression of these genes was evaluated using publicly available transcriptomic COVID-19 whole transcriptomic and single-cell datasets of samples obtained from bronchioalveolar fluid (BALF), lung autopsies, and whole blood of COVID-19 patients with different disease severity. We also compared between the blood

Table 1
Pro-oxidant gene signatures.

Gene	Approved name	HGNC ID	Location
ACOX1	acyl-CoA oxidase 1	HGNC:119	17q25.1
ACOX3	acyl-CoA oxidase 3, pristanoyl	HGNC:121	4p16.1
AOC1	amine oxidase copper containing 1	HGNC:80	7q36.1
AOC2	amine oxidase copper containing 2	HGNC:549	17q21.31
AOC3	amine oxidase copper containing 3	HGNC:550	17q21.31
AOX1	aldehyde oxidase 1	HGNC:553	2q33.1
CYBA	cytochrome *b*-245 alpha chain	HGNC:2577	16q24.2
CYBB	cytochrome *b*-245 beta chain	HGNC:2578	Xp21.1-p11.4
DAO	D-amino acid oxidase	HGNC:2671	12q24.11
DDO	D-aspartate oxidase	HGNC:2727	6q21
DUOX1	dual oxidase 1	HGNC:3062	15q21.1
DUOX2	dual oxidase 2	HGNC:13,273	15q21.1
GFER	growth factor, augmenter of liver regeneration	HGNC:4236	16p13.3
HAO1	hydroxyacid oxidase 1	HGNC:4809	20p12.3
HAO2	hydroxyacid oxidase 2	HGNC:4810	1p12
IL4I1	interleukin 4 induced 1	HGNC:19,094	19q13.33
LOX	lysyl oxidase	HGNC:6664	5q23.1
MAOA	monoamine oxidase A	HGNC:6833	Xp11.3
MAOB	monoamine oxidase B	HGNC:6834	Xp11.3
MPO	myeloperoxidase	HGNC:7218	17q22
NCF2	neutrophil cytosolic factor 2	HGNC:7661	1q25.3
NOS1	nitric oxide synthase 1	HGNC:7872	12q24.22
NOS2	nitric oxide synthase 2	HGNC:7873	17q11.2
NOS3	nitric oxide synthase 3	HGNC:7876	7q36.1
NOX1	NADPH oxidase 1	HGNC:7889	Xq22.1
NOX3	NADPH oxidase 3	HGNC:7890	6q25.3
NOX4	NADPH oxidase 4	HGNC:7891	11q14.3
NOX5	NADPH oxidase 5	HGNC:14,874	15q23
PAOX	polyamine oxidase	HGNC:20,837	10q26.3
PCYOX1	prenylcysteine oxidase 1	HGNC:20,588	2p13.3
PIPOX	pipecolic acid and sarcosine oxidase	HGNC:17,804	17q11.2
PNPO	pyridoxamine 5′-phosphate oxidase	HGNC:30,260	17q21.32
QSOX1	quiescin sulfhydryl oxidase 1	HGNC:9756	1q25.2
QSOX2	quiescin sulfhydryl oxidase 2	HGNC:30,249	9q34.3
SMOX	spermine oxidase	HGNC:15,862	20p13
SUOX	sulfite oxidase	HGNC:11,460	12q13.2

Table 2
Oxidative responsive gene signatures.

Gene	Approved name	HGNC ID	Location
ANGPTL7	angiopoietin like 7	HGNC:24,078	1p36.22
APOA4	apolipoprotein A4	HGNC:602	11q23.3
APTX	Aprataxin	HGNC:15,984	9p21.1
ATOX1	antioxidant 1 copper chaperone	HGNC:798	5q33.1
CYGB	cytoglobin	HGNC:16,505	17q25.1
CYP1A1	cytochrome P450 family 1 subfamily A member 1	HGNC:2595	15q24.1
DGKK	diacylglycerol kinase kappa	HGNC:32,395	Xp11.22
DHCR24	24-dehydrocholesterol reductase	HGNC:2859	1p32.3
DUSP1	dual specificity phosphatase 1	HGNC:3064	5q35.1
GCLM	glutamate-cysteine ligase modifier subunit	HGNC:4312	1p22.1
GLRX2	glutaredoxin 2	HGNC:16,065	1q31.2
IPCEF1	interaction protein for cytohesin exchange factors 1	HGNC:21,204	6q25.2
MGST1	microsomal glutathione S-transferase 1	HGNC:7061	12p12.3
MSRA	methionine sulfoxide reductase A	HGNC:7377	8p23.1
MT1X	metallothionein 1X	HGNC:7405	16q13
NFE2L2	nuclear factor, erythroid 2 like 2	HGNC:7782	2q31.2
NFIX	nuclear factor I X	HGNC:7788	19p13.13
NFKB1	nuclear factor kappa B subunit 1	HGNC:7794	4q24
NUDT1	nudix hydrolase 1	HGNC:8048	7p22.3
OXSR1	oxidative stress responsive kinase 1	HGNC:8508	3p22.2
PDLIM1	PDZ and LIM domain 1	HGNC:2067	10q23.33
PNKP	polynucleotide kinase 3′-phosphatase	HGNC:9154	19q13.33
PRNP	prion protein	HGNC:9449	20p13
RNF7	ring finger protein 7	HGNC:10,070	3q23
S100A7	S100 calcium binding protein A7	HGNC:10,497	1q21.3
S100A8	S100 calcium binding protein A8	HGNC:10,498	1q21.3
S100A9	S100 calcium binding protein A9	HGNC:10,499	1q21.3
SCARA3	scavenger receptor class A member 3	HGNC:19,000	8p21.1
SGK2	serum/glucocorticoid regulated kinase 2	HGNC:13,900	20q13.12
SGK3	serum/glucocorticoid regulated kinase family member 3	HGNC:10,812	8q13.1
SP1	Sp1 transcription factor	HGNC:11,205	12q13.13
SRXN1	sulfiredoxin 1	HGNC:16,132	20p13
STK25	serine/threonine kinase 25	HGNC:11,404	2q37.3

Table 3
Antioxidant gene signatures.

Approved symbol	Approved name	HGNC ID	Location
CAT	Catalase	HGNC:1516	11p13
CTH	cystathionine gamma-lyase	HGNC:2501	1p31.1
DRD1	dopamine receptor D1	HGNC:3020	5q35.2
DRD2	dopamine receptor D2	HGNC:3023	11q23.2
DRD3	dopamine receptor D3	HGNC:3024	3q13.31
DRD4	dopamine receptor D4	HGNC:3025	11p15.5
DRD5	dopamine receptor D5	HGNC:3026	4p16.1
ERCC1	ERCC excision repair 1, endonuclease non-catalytic subunit	HGNC:3433	19q13.32
ERCC2	ERCC excision repair 2, TFIIH core complex helicase subunit	HGNC:3434	19q13.32
ERCC3	ERCC excision repair 3, TFIIH core complex helicase subunit	HGNC:3435	2q14.3
ERCC6	ERCC excision repair 6, chromatin remodeling factor	HGNC:3438	10q11.23
ERCC8	ERCC excision repair 8, CSA ubiquitin ligase complex subunit	HGNC:3439	5q12.1
FGF5	fibroblast growth factor 5	HGNC:3683	4q21.21
FOS	Fos proto-oncogene, AP-1 transcription factor subunit	HGNC:3796	14q24.3
GCLC	glutamate-cysteine ligase catalytic subunit	HGNC:4311	6p12.1
GPX1	glutathione peroxidase 1	HGNC:4553	3p21.31
GPX3	glutathione peroxidase 3	HGNC:4555	5q33.1
GPX4	glutathione peroxidase 4	HGNC:4556	19p13.3
GSR	glutathione-disulfide reductase	HGNC:4623	8p12
GSS	glutathione synthetase	HGNC:4624	20q11.22
GSTA1	glutathione S-transferase alpha 1	HGNC:4626	6p12.2
GSTM1	glutathione S-transferase mu 1	HGNC:4632	1p13.3
GSTM3	glutathione S-transferase mu 3	HGNC:4635	1p13.3
GSTP1	glutathione S-transferase pi 1	HGNC:4638	11q13.2
GSTT1	glutathione S-transferase theta 1	HGNC:4641	22q11.23
GSTT2	glutathione S-transferase theta 2 (gene/pseudogene)	HGNC:4642	22q11.23
HMOX1	heme oxygenase 1	HGNC:5013	22q12.3
HMOX2	heme oxygenase 2	HGNC:5014	16p13.3
JUNB	JunB proto-oncogene, AP-1 transcription factor subunit	HGNC:6205	19p13.13
MAPK10	mitogen-activated protein kinase 10	HGNC:6872	4q21.3
MAPK14	mitogen-activated protein kinase 14	HGNC:6876	6p21.31
MTHFR	methylenetetrahydrofolate reductase	HGNC:7436	1p36.22
NDUFA12	NADH: ubiquinone oxidoreductase subunit A12	HGNC:23,987	12q22
NDUFA6	NADH: ubiquinone oxidoreductase subunit A6	HGNC:7690	22q13.2
NDUFB4	NADH: ubiquinone oxidoreductase subunit B4	HGNC:7699	3q13.33
NDUFS2	NADH: ubiquinone oxidoreductase core subunit S2	HGNC:7708	1q23.3
NDUFS8	NADH: ubiquinone oxidoreductase core subunit S8	HGNC:7715	11q13.2
NQO1	NAD(P)H quinone dehydrogenase 1	HGNC:2874	16q22.1
PARK7	Parkinsonism associated deglycase	HGNC:16,369	1p36.23
PON1	paraoxonase 1	HGNC:9204	7q21.3
PON2	paraoxonase 2	HGNC:9205	7q21.3
PPARGC1A	PPARG coactivator 1 alpha	HGNC:9237	4p15.2
PRDX2	peroxiredoxin 2	HGNC:9353	19p13.13
PRDX5	peroxiredoxin 5	HGNC:9355	11q13.1
PRDX6	peroxiredoxin 6	HGNC:16,753	1q25.1
SELENOP	selenoprotein P	HGNC:10,751	5p12
SELENOS	selenoprotein S	HGNC:30,396	15q26.3
SESN2	sestrin 2	HGNC:20,746	1p35.3
SOD1	superoxide dismutase 1	HGNC:11,179	21q22.11
SOD2	superoxide dismutase 2	HGNC:11,180	6q25.3
SOD3	superoxide dismutase 3	HGNC:11,181	4p15.2
TXN	thioredoxin	HGNC:12,435	9q31.3
TXN2	thioredoxin 2	HGNC:17,772	22q12.3
TXNRD1	thioredoxin reductase 1	HGNC:12,437	12q23.3
TXNRD2	thioredoxin reductase 2	HGNC:18,155	22q11.21
UCP2	uncoupling protein 2	HGNC:12,518	11q13.4

oxidative stress gene expression levels of COVID-19 and three respiratory infections: SARS-COV-1, influenza (IAV), and respiratory syncytial virus (RSV). These datasets were publicly available at National Center for Biotechnology Information Gene Expression Omnibus (NCBI GEO, http://www.ncbi.nlm.nih.gov/geo) and the European Bioinformatics Institute (EMBL-EBI, https://www.ebi.ac.uk) were used.

The datasets used is detailed in Table 4. RNA-sequencing platforms were used for COVID-19 studies, while microarray platforms were used for older datasets of SARS-COV-1, IAV, and RSV (Table 4). For the COVID-19 lung autopsies dataset (PRJNA646224) [32], the investigators extracted RNA from Formalin fixed paraffin embedded lung tissues of 9 COVID-19 fatal cases, and 10 SARS-COV-2-uninfected individuals who undertook biopsy as part of routine clinical care for lung cancer. For this lung autopsy datasets, we used processed sequencing data provided by Wu Meng et al. [32].

For COVID-19 whole blood transcriptomic dataset, we used processed sequencing data deposited under project number EGAS00001004503 [33]. In this study, Aschenbrenner et al. extracted whole blood RNA from 10 controls, 20 severe and 19 mild COVID-19 patients and analyzed it using NovaSeq 6000 [34].

To validate whole blood and lung autopsies findings, the expression of the shared oxidative stress genes was extracted from a third COVID-19 leucocyte dataset (GEO: GSE157103) consisting of 37 severe COVID-19 and 51 non-severe COVID-19 patients [34]. COVID-19 disease severity was defined by intensive care unit (ICU) admission, while burden of co-morbidity was obtained by measuring the Charlson Comorbidity Index score [35]. Logistic regression analysis was then used to determine the independent association between expression of oxidative stress genes and COVID-19 disease severity. ICU admission factor was used as

Table 4
Gene expression datasets used in this study.

Groups	GEO accession	Platform	Sample	Condition 1	Condition 2
	GSE1739 (38)	GPL201	PBMCs	Controls (n = 4)	SARS-COV-1 (n = 10)
	GSE17156 (37)	GPL571	Whole blood	Controls (n = 17)	Influenza H3N2 (n = 17)
	GSE17156 (37)	GPL571	Whole blood	Controls (n = 20)	Respiratory syncytial virus (n = 20)
RNA-seq Data					
	PRJNA646224 (32)	GPL21697	Lung autopsies	Controls (n = 10)	Lung autopsies (n = 9)
	EGAS00001004503 (33)	GPL24676	Whole blood	Controls (n = 10)	COVID -19 (n = 39)
	GSE157103 (34)	GPL24676	Leukocytes from whole blood	Controls (n = 10)	Non-severe COVID-19 (n = 51), severe COVID-19 (n = 37)
	GSE147507 (6)	GPL18573	Primary human lung epithelium (NHBE)	Mock infected NHBE	IAV (n = 4) and SARS-COV-2 (n = 3) infected NHBE
Single-cell RNA-seq Data					
	GSE145926 (8)	GPL23227	Bronchoalveolar lavage fluid	Healthy (n = 6)	Moderate (n = 3) and Severe (n = 6) COVID-19
	GSE150728 (40)	GPL24676	Peripheral blood mononuclear cells	Healthy (n = 6)	Severe COVID-19 (n = 7)

IAV, Influenza A virus; SARS-COV, Severe acute respiratory syndrome coronavirus.

the dependent factor and oxidative stress gene expression as independent factor. The model was adjusted for age, gender, body mass index and Charlson Comorbidity Index score [35]. Statistical analyses were performed using R software (v 3.0.2), SPSS 25.00 (SPSS Inc., Chicago, IL, USA), and Prism (v8; GraphPad Software). P-value of <0.05 considered statistically significant.

We also examined how SARS-COV-2 and IAV infection may regulate the expression of oxidative stress genes in whole blood and lung autopsies. We, hence, reanalyzed the data deposited by Daniel Blanco-Melo (GEO: GSE147507) [6] to compare the expression of these genes in viral-infected lung epithelial cells compared to Mock-infected controls. For leucocyte datasets (GEO: GSE157103) and Daniel Blanco-Melo (GEO: GSE147507)), we processed the RNAseq raw count using the Bioconductor package limma-voom [36], and presented the results as log2 counts per million (log CPM). Log-transformed normalized intensities were also used in Linear Models for MicroArray data (LIMMA) analyses to identify differentially expressed genes between diseased and control groups.

Transcriptomic datasets of peripheral blood mononuclear cells (PBMCs) isolated from RSV and IAV infected patients (GEO: GSE17156) [37] and from SARS-COV-1 infected patients (GEO: GSE1739) [38] were analyzed. In both studies, blood was obtained during peak of patient's symptoms, and processed by the investigators for RNA extraction and hybridization following Affymetrix protocol. After quality check, we normalized, and log transformed the raw Affymetrix data. Microarray data (CEL files) were pre-processed in our study with Robust Multi-Array Average (RMA) technique using R software [39]. The probe set with the largest interquartile range (IQR) of expression values was selected to represent the gene. Raw data from different studies was never mixed or combined. For each study, the fold change was obtained separately by analyzing data of diseased and controls.

Single-cell RNA sequencing datasets were obtained from two studies on BALF and PBMCs COVID-19 samples. In the first study, Liao et al. performed single-cell RNA sequencing on BALF obtained from 6 severe and 3 moderate COVID-19 patients and 3 healthy control [8]. The investigators clustered macrophages into four groups based on the expression of the differentiation markers. Group one and two represented M1-like macrophages, while group three represented M2-like macrophages [8]. Fold changes were generated for each group of macrophages relative to the total macrophage population. In addition, the differential gene expression of $CD8^+$ T cells was compared between moderate and severe groups. For the second study, single cell dataset of neutrophils sorted from PBMCs were used [40]. Wilk, AJ et al. performed single sequencing on blood neutrophils from 7 COVID-19 patients, and 6 six healthy controls [40]. The investigators clustered neutrophils into two clusters, low-density neutrophils and canonical neutrophils. The novel cell population of low-density neutrophils was significantly increased only in patients with ARDs.

For the purpose of these two investigations, we used the published processed data. The details of sample isolation, sequencing, and data processing are available at NCBI GEO, and the protocol of each study [8, 40]. Briefly, single-cell RNA-seq libraries were generated and cellranger 10X genomics was used to generate fastq files from the sequenced data, the reads were aligned to the human reference genome (GRCh38; 10x cellranger reference GRCh38 v3.0.0). Further filtering and normalization were performed using Seurat R package v3.1.5 [17]. Model-based analysis of single cell transcriptomics (MAST) algorithm in Seurat v3 was used to identify differentially expressed genes (DEGs) and to determine the fold change. Only DEGs with a two-sided p value < 0.05 adjusted for multiple comparisons by Bonferroni's correction were selected.

2.1. qRT-PCR

Saliva was obtained from 5 uninfected controls (average age of 34 ± 8 years), 7 asymptomatic COVID-19 patients (average age of 44 ± 6 years), and 10 severe COVID-19 patients (average age of 53 ± 11 years). Blood samples were obtained from 5 uninfected controls (average age of 34 ± 8 years), 9 asymptomatic COVID-19 patients (average age of 43 ± 6 years), and 10 severe COVID-19 patients (average age of 56 ± 11 years). COVID-19 cases were confirmed by qRT-PCR positive test, while the uninfected donor controls were confirmed by qRT-PCR negative test. This study was approved by Dubai Scientific Research Ethics Committee (DSREC). Written, informed consents were obtained from all study participants prior to inclusion. Precautions recommended by CDC for safe collecting, handling and testing of biological fluids were followed [41].

Total RNA from whole blood and saliva was isolated using Trizol reagent according to the manufacturer's instructions (Invitrogen, Carlsbad, CA) [42]. Complementary cDNA was synthesized from 1 μg of RNA using the High-Capacity cDNA Reverse Transcription Kit (Applied Biosystems) according to the manufacturer's protocol. For cDNA amplification, 5x Hot FirePol EvaGreen qRT-PCR SuperMix (Solis Biodyne) was used, and qRT-PCR was performed in QuantStudio 3 Real-Time PCR System (Applied Biosystems) [43]. Primer sequences for MPO, S100A8, S100A9, and 18s used in qRT-PCR are deposited in Supplementary Table 1. Gene expression was analyzed using the Comparative Ct (ΔΔCt) method upon normalization to the reference gene 18s rRNA [44]. The data was log transformed. Unpaired student t-test was used to compare between the independent groups. (GraphPad Software, San Diego, Calif). For all analyses, P-values <0.05 were considered significant.

3. Results

3.1. Expression of oxidative stress genes is increased in blood and lung tissue during SARS-COV-2 infection relative to disease severity

Using publicly available transcriptomic datasets, we have determined the expression levels of 125 oxidative stress genes, including 37

pro-oxidant genes, 32 oxidative-responsive genes, and 56 antioxidant genes. The lists of these genes are presented in Tables 1–3 The datasets used in this study are presented in Table 4. Expression levels of the oxidative stress genes were determined in lung autopsies and whole blood of COVID-19 patients (Fig.1 and Supplementary Fig. 1). For whole blood, RNA-sequencing data was extracted from 20 severe COVID-19 patients and 10 controls (Fig. 1A). For lung, RNA-sequencing data was obtained from 9 deceased COVID-19 patients and 10 negative controls (PRJNA646224) (Fig. 1B). Twenty-six oxidative stress genes were upregulated in whole blood, while only 10 genes in lung autopsies (Fig. 1C). Seven of these genes were commonly upregulated in both whole blood and lung autopsies (Fig. 1C), including the following five pro-oxidants/oxidative responsive genes: Myeloperoxidase (MPO), Calprotectin (S100A8/S100A9), Sulfiredoxin-1 (SRXN1), Glutamate-cysteine ligase modifier (GCLM), and two antioxidant genes: Sestrin 2 (SESN2) and Thioredoxin (TXN) (Fig. 1C). A significant increase in lung tissue expression of S100A8 (4.2 ± 0.3 log-fold vs 2.7 ± 0.3 log-fold; p-value = 0.001) and SRXN1 (2.1 ± 0.2 log-fold vs 1.04 ± 0.4 log-fold; p-value = 0.03) compared to whole blood was observed (Fig. 1C). We then determined the expression of these seven shared genes in NHBE infected with IAV or SARS-COV-2 using data deposited by Daniel Blanco-Melo (GEO: GSE147507) [6]. Of these seven genes, SRXN1 and SESN2 were slightly increased in IAV infected NHBE (n = 4 IAV NHBE vs n = 4 mock infected NHBE), while calprotectin genes of S100A8 (log-fold of 1.9 ± 0.15; p-value < 0.0001) and S100A9 (log-fold of 1.1 ± 0.07; p-value < 0.0001) were noticeably increased in SARS-COV-2 infected NHBE (n = 3 SARS–CO–V-2 NHBE vs n = 3 mock infected NHBE, GEO: GSE147507). The in-vitro infected results are displayed in Fig. 1D.

To confirm this increase in expression of oxidative genes during COVID-19 infection, we also determined the expression of these seven genes in a transcriptome dataset of leucocyte isolated from 37 severe and 51 non-severe COVID-19 patients (GSE157103). Confirming the previous results, this analysis showed a significant upregulation of the selected seven oxidative stress genes in severe versus non-severe COVID-19 (Fig. 2). To further characterize the association between expression of these genes and COVID-19 severity we carried a logistic regression analysis. After adjustment with age, gender, body mass index, and Charlson Comorbidity Index score, the expression of these seven genes were significantly associated with COVID-19 severity and ICU admission. (Supplementary Table 2).

3.2. *Expression of oxidative stress genes is upregulated in lung tissue inflammatory cells during COVID-19 infection*

After establishing an overall upregulation of oxidative stress genes in autopsies of COVID-19 patients, we next determined whether the observed increase in oxidative stress is reflected on the main inflammatory cells regulating COVID-19 severity. A single cell dataset of macrophage and $CD8^+$ cells isolated from bronchioalveolar fluid (GEO: GSE145926) of COVID-19 severe patients was used [8]. In this study, macrophages were clustered into four main groups. Group one and two represented M1-like macrophages and group three represented M2-like

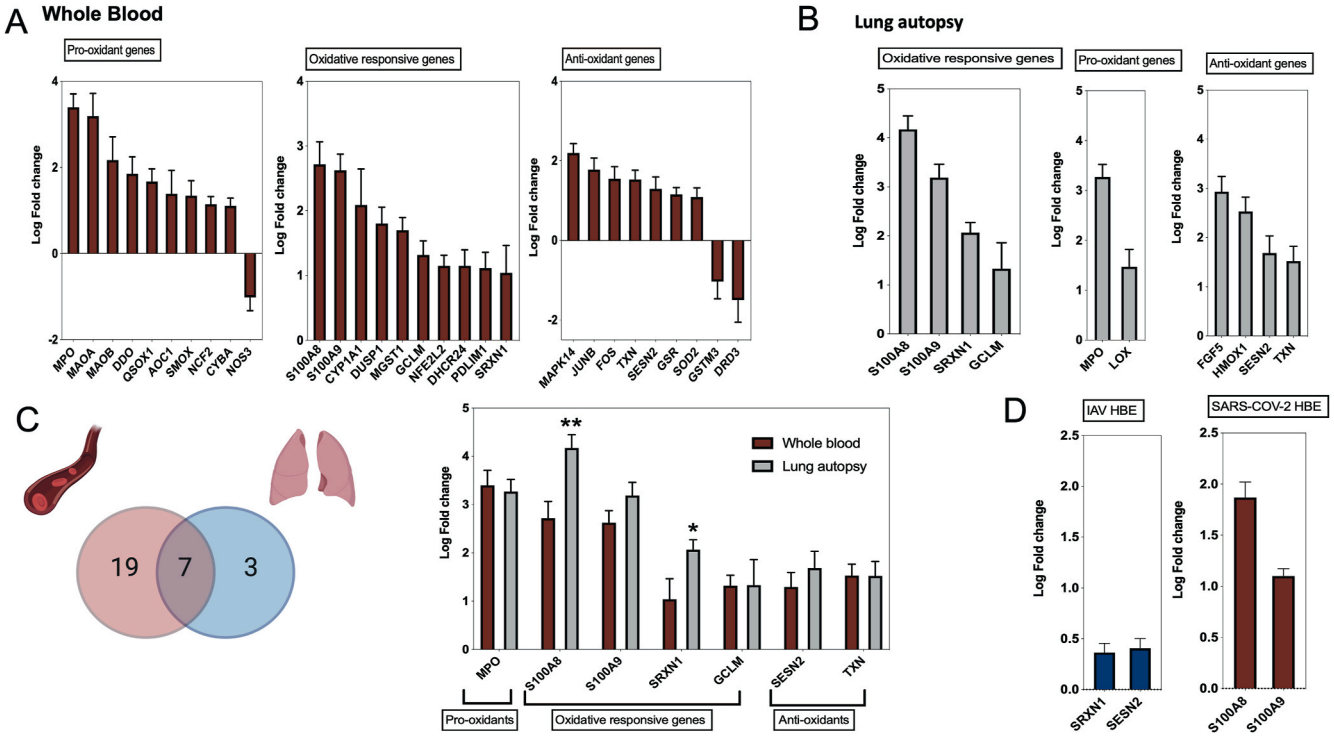

Fig. 1. Oxidative stress gene expression in whole blood and lung autopsies of COVID-19 patients. (A) Expression of 26 oxidative genes were upregulated in whole blood of severe COVID-19 vs non-infected controls. Whole blood transcriptomic data set was used (n = 20 severe COVID-19 vs n = 10 controls, dataset: EGAS00001004503). Results are presented as fold change of gene expression between cases and controls. (B) Upregulation of 10 oxidative genes in lung autopsies (n = 9 COVID-19 vs n = 10 controls, dataset: PRJNA646224). Results are presented as fold change of gene expression between cases and controls. (C) Seven oxidative stress genes were shared between whole blood and lung autopsies. MPO, S100A8, and S100A9 were among the top upregulated oxidative genes, while S100A8 and SRXN1 were higher in lung autopsies. Results are presented as fold change of gene expression between cases and controls. Unpaired student t-test was used to compare between fold changes in mild and severe COVID-19. *p < 0.05, **p < 0.01, ***p < 0.001, ****p < 0.0001. (D) The seven shared oxidative genes were analyzed in SAR-COV-2 and influenza A virus infected human lung epithelial cells. Independent biological replicates of primary human lung epithelium (NHBE) were mock treated or infected with SARS-COV-2 (USA-WA1/2020), or IAV (A/Puerto Rico/8/1934 (H1N1)). Of these seven genes, SRXN1 and SESN2 were slightly increased in IAV infected NHBE (n = 4 IAV NHBE vs n = 4 mock infected NHBE, GEO: GSE147507), while calprotectin genes of S100A8 and S100A9 were noticeably increased in SARS-COV-2 infected NHBE (n = 3 SARS–CO–V-2 NHBE vs n = 3 mock infected NHBE, GEO: GSE147507). All fold changes presented in the figure were significant with a p value < 0.05.

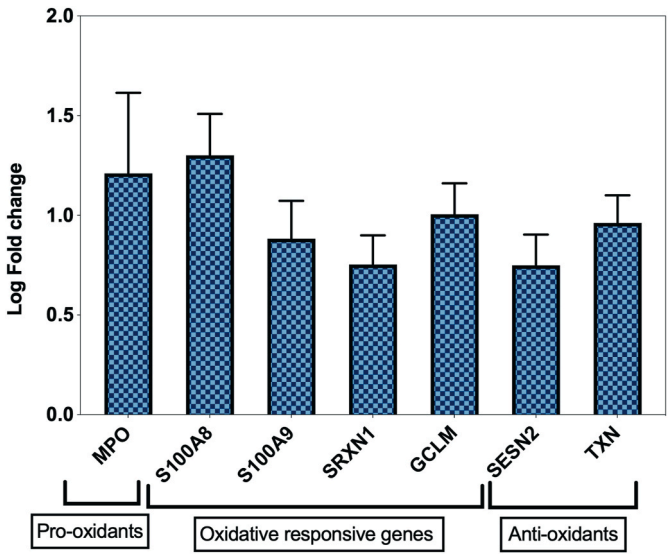

Fig. 2. Upregulation of common oxidative genes in leucocytes of severe COVID-19 patients. The seven shared oxidative genes between autopsy and whole blood COVID-19 samples were found to be higher in leucocytes of severe COVID-19 (n = 37 Severe vs n = 51 non-severe COVID-19, GSE157103). All fold changes presented in the figure were significant with a p value < 0.05.

macrophages; M1 and M2 like macrophages were more prominent in severe COVID-19. The fourth group was found to be more common in healthy and non-severe COVID-19 patients [8]. Interestingly, M1 and M2 macrophages of severe COVID-19 patients had an overall increase in the expression of pro-oxidant, oxidative responsive, and antioxidant genes, while macrophages from non-severe COVID-19 and healthy individuals showed more increase in antioxidants genes. Among oxidative genes, the expression of S100A8 (1.8 log-fold; p-value <0.0001) and S100A9 (1.5 log-fold; p-value <0.0001) was significantly increased (Fig. 3A). Further, a distinct upregulation of oxidative stress genes in BALF $CD8^+$ T cells isolated from the same severe COVID-19 patients, while these markers were not changed in BALF $CD8^+$ T cells isolated from non-severe COVID-19 patients (Fig. 3B). All fold changes presented in Fig. 3A and B were significant with a p value < 0.05.

Neutrophils are one of the main sources of the oxidative stress genes and a key inflammatory cell regulating COVID-19 pathogenesis. To determine the expression of oxidative stress genes within the neutrophils, a single cell dataset of immune cells isolated from PBMCs (GEO: GSE150728) of COVID-19 severe patients was used [40]. In this study overall neutrophil counts were increased in severe COVID-19, while presence of low-density neutrophils was associated with severe COVID-19 phenotype and development of ARDS [40]. Low-density neutrophils showed upregulation of MPO (1.6 log-fold; p-value <0.0001), CYBB (1.1 log-fold; p-value <0.0001), S100A8 (0.8 log-fold; p-value <0.0001) and S100A9 (0.34 log-fold; p-value <0.0001) calprotectin genes. Noticeably, antioxidant genes of JUNB (−0.7 log-fold; p-value <0.0001), FOS (−1.1 log-fold; p-value <0.0001), and SOD2

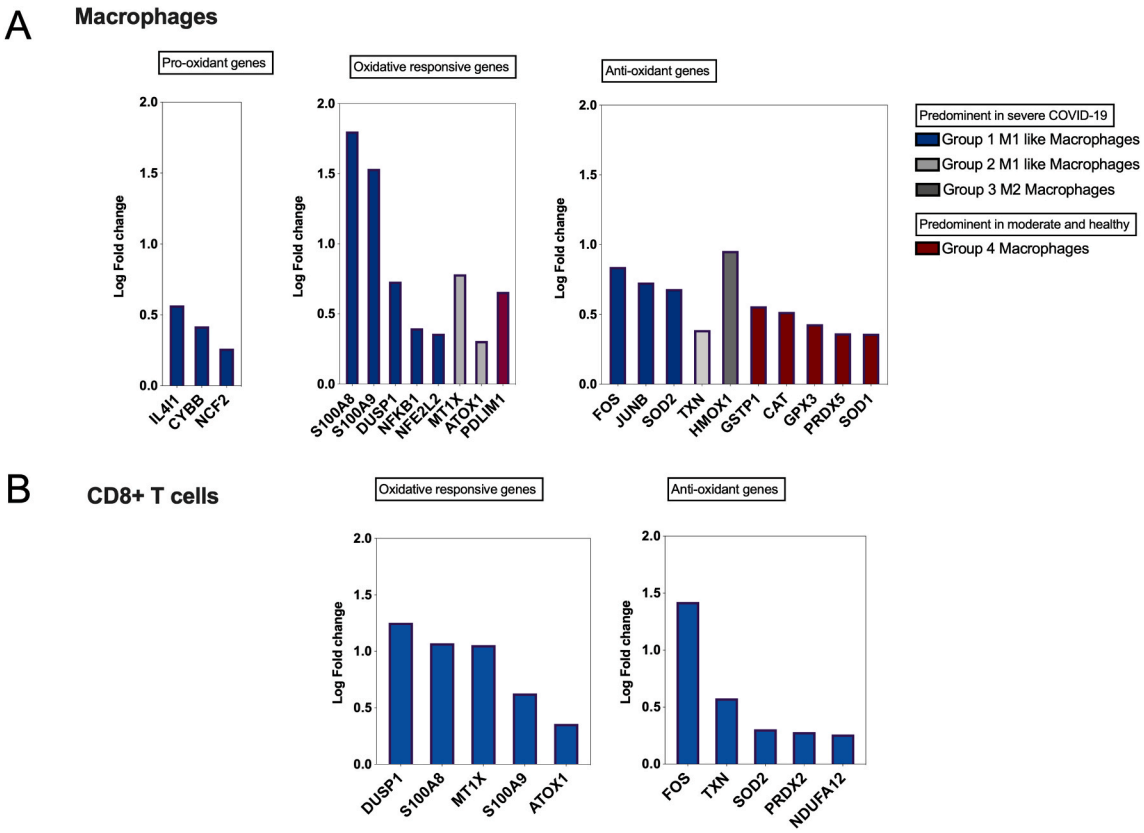

Fig. 3. Single-cell expression data of bronchoalveolar lavage from patients with COVID-19 (GEO: GSE145926). Single-cell RNA sequencing was performed on bronchoalveolar lavage fluid (BALF) from 6 severe and 3 moderate COVID-19 patients and 3 healthy control. (A) Prominent upregulation of S100A8 and S100A9 in M1 macrophage group. Macrophages were clustered into four groups; M1 macrophages were presented with group 1 and 2, while M2 macrophages were presented with group 3. Both M1 and M2 like macrophages were enriched in severe COVID-19. Group 4 macrophages were predominant in moderate and healthy controls and presented the less severe COVID-19. Fold changes were generated for each group of macrophages relative to total macrophages. (B) Specific upregulation of oxidative stress genes in $CD8^+$ T cells from severe COVID-19 patients, while none of the oxidative genes appeared in the non-severe COVID-19 cluster. All fold changes presented in the figure were significant with a p value < 0.05.

(−1.5 log-fold; p-value <0.0001) were found to be downregulated, suggesting increase of pro-oxidant and decrease of antioxidant signatures within these neutrophils at the critical ARDS and COVID-19 severe stage (Supplementary Fig. 2).

3.3. Myeloperoxidase and calprotectin levels are upregulated in saliva of COVID-19 patients relative to disease severity

We next examined whether the observed increase in these oxidative stress genes can be detected in saliva of COVID-19 patients. This may hence suggest the usage of these genes as non-invasive biomarkers for disease severity. To do that, we first validated the increase of these markers in blood of asymptomatic and severe COVID-19 patients using qRT-PCR. A significant increase in blood levels of MPO and calprotectin in severe versus asymptomatic COVID-19 patients was observed (Fig. 4A). MPO was increased one log-fold more in severe versus asymptomatic (p-value = 0.0033), while log-fold difference in S100A8 and S100A9 were 0.87 log-fold (p-value 0.004) and log-fold 0.9 (p-value = 0.006), respectively. We then determined the level of these genes in saliva from the same COVID-19 patients (Fig. 4B). This increase was comparable in saliva compared to blood samples which may suggest that saliva level of expression of these genes could reflect the level of COVID-19 severity. In severe versus asymptomatic saliva, the log-fold difference was one log-fold (p-value = 0.0001) for MPO, 2.7 log-fold (p-value<0.0001) for S100A8, and 0.3 log-fold (p-value = 0001) for S100A9.

3.4. Prominent upregulation of oxidative stress genes during coronavirus infections relative to other viral infections

We next compared the profile of enhanced oxidative stress gene expression observed during SARS-COV-2 to that detected during other respiratory viral infections. To do that, we used transcriptomic microarrays and RNA-sequencing data of PBMCs isolated from SARS-COV-1, IAV, and RSV infected patients at the peak of disease. For each condition, differential gene expression was obtained by comparing the normalized gene expression of the infected group to those of healthy donors (Fig. 5A). For IAV and RSV infections, none of the oxidative stress genes were increased more than one log fold-change (FC), while 7 genes for SARS-COV-1 and 27 genes for SARS-COV-2 infections were upregulated to a than one log FC (Fig. 5A). TXN, QSOX1, MAPK14, MPO, S100A9, and S100A8 were the top shared oxidative stress genes appearing in both coronavirus respiratory infections, with an increase in expression of more than 1.5 folds following infection (Fig. 5B).

4. Discussion

Herein, the dysregulation in the expression levels of 125 oxidative stress genes during severe COVID-19 viral infection was explored using bioinformatic analysis of publicly available transcriptomic datasets of lung autopsies, bronchioalveolar fluid, and blood from SARS-COV-2 infected individuals. Seven oxidative stress genes were found to be upregulated in whole blood and lung autopsies of severe COVID-19 (MPO, S100A8, S100A9, SRXN1, GCLM, SESN2, and TXN) (Fig. 1C). Of these genes, calprotectin genes, S100A8 and S100A9, were distinctly elevated in NHBE infected with SARS-COV-2 as compared to cells infected with IAV (Fig. 1D). We then examined if the increase in these genes was relative to disease severity. These genes were significantly increased in blood leucocytes of severe compared to non-severe COVID-19 (Fig. 2). Using logistic regression, this association remained significant even after adjustment with cofounding factors of age, gender, body mass index, and Charlson Comorbidity Index score (Supplementary Table 2).

Similarly, using single cell BALF transcriptomics, the expression of the oxidative genes was shown to be increased more in macrophages and $CD8^+$ T cells from severe COVID-19 patients compared to non-severe and healthy uninfected donors. Results from single cell transcriptomic

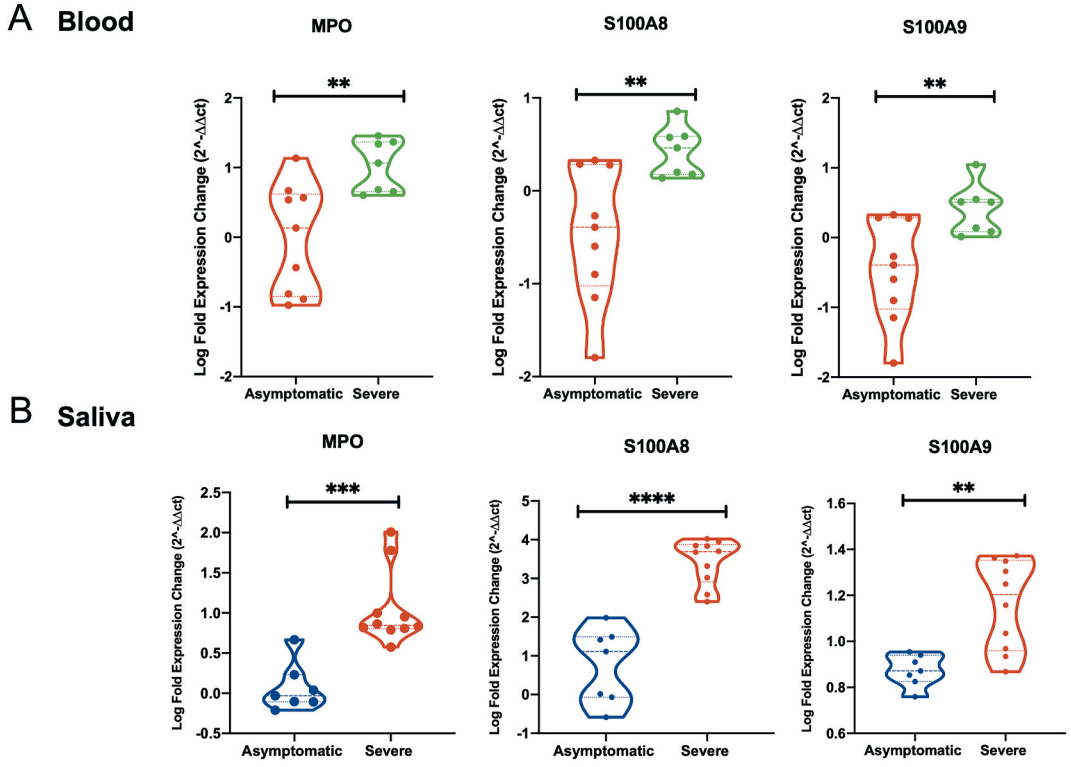

Fig. 4. Myeloperoxidase and calprotectin levels are upregulated in saliva of COVID-19 patients relative to disease severity. (A) Gene expression level of MPO, S100A8 and S100A9 was higher in blood from severe COVID-19 (n = 7) as compared to asymptomatic COVID-19 (n = 9). (B) Gene expression level of MPO, S100A8 and S100A9 was higher in saliva from severe COVID-19 (n = 10) as compared to asymptomatic COVID-19 (n = 7). Results are presented as log2 fold change. Unpaired student t-test was used to compare between the independent groups. *p < 0.05, **p < 0.01, ***p < 0.001, ****p < 0.0001.

A

SARS-COV-2

Pro-oxidant		
Gene	*log FC*	*p-value*
MPO	3.40	0.000
MAOA	3.19	0.000
MAOB	2.17	0.000
DDO	1.85	0.000
QSOX1	1.67	0.000
AOC1	1.39	0.002
SMOX	1.34	0.000
NCF2	1.15	0.000
CYBA	1.11	0.000
NOS3	-1.02	0.005
Oxidative responsive gene		
Gene	*log FC*	*p-value*
S100A8	2.72	0.000
S100A9	2.62	0.000
CYP1A1	2.09	0.000
DUSP1	1.80	0.000
MGST1	1.70	0.000
GCLM	1.32	0.000
NFE2L2	1.15	0.000
DHCR24	1.15	0.000
PDLIM1	1.12	0.000
SRXN1	1.04	0.012
Antioxidant		
Gene	*log FC*	*p-value*
MAPK14	2.19	0.000
JUNB	1.78	0.000
FOS	1.55	0.000
TXN	1.53	0.000
SESN2	1.29	0.000
GSR	1.16	0.000
SOD2	1.09	0.000
GSTM3	-1.04	0.017
DRD3	-1.50	0.008

SARS-COV-1

Pro-oxidant		
Gene	*log FC*	*p-value*
MPO	3.79	0.000
QSOX1	1.61	0.002
Oxidative responsive gene		
Gene	*log FC*	*p-value*
S100A9	1.49	0.016
MSRA	1.38	0.005
S100A8	1.32	0.013
Antioxidant		
Gene	*log FC*	*p-value*
TXN	1.30	0.001
MAPK14	1.22	0.034
ERCC3	-0.65	0.045
DRD2	-1.04	0.011
GCLC	-1.11	0.001

IAV

Pro-oxidant		
Gene	*log FC*	*p-value*
CYBB	0.53	0.000
AOC2	-0.54	0.001
AOC3	-0.67	0.000
Oxidative responsive gene		
Gene	*log FC*	*p-value*
MT1X	0.86	0.000
GLRX2	0.64	0.000
ATOX1	0.58	0.000

RSV

Antioxidant		
Gene	*log FC*	*p-value*
TXN	0.51	0.000

B

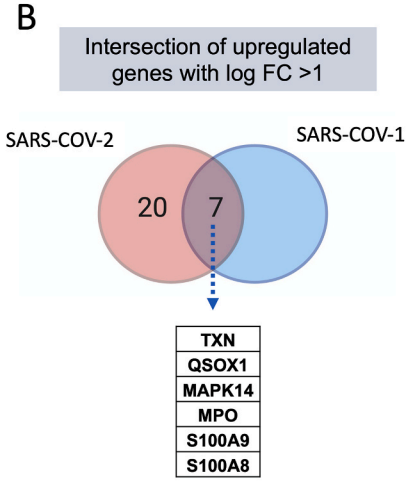

Fig. 5. Expression of oxidative stress genes during SARS-COV-2 and other viral infections. The number and intensity of gene upregulation were higher during SARS-COV-2 infection compared to other respiratory viral infection. (A) Upregulation of oxidative stress genes during different respiratory infections. The difference in gene expression of case and controls is provided as fold change. (B) Intersection of upregulated oxidative signatures in coronavirus infections; SARS-COV-1 and SARS-COV-2. The following datasets were used; GSE17156 (n = 17 IAV vs n = 17 controls), GSE17156 (n = 20 RSV vs n = 20 controls), GSE1739 (n = 10 SARS-COV-1 vs n = 4 controls), and EGAS00001004503 (n = 39 COVID-19 vs n = 10 controls). For all analyses, $p < 0.05$ was considered significant. IAV, influenza A virus; RSV, Respiratory syncytial virus.

of blood neutrophils revealed an increase in both canonical and low-density neutrophil during SARS-COV-2 infection. This increase was more apparent in severe COVID-19 disease and was characterized by upregulation of the expression of MPO, and calprotectin genes, while the antioxidant genes were found to be downregulated.

Severe COVID-19 disease has been associated with innate immune dysregulation, an increased neutrophil-to-lymphocyte ratio, lymphopenia, and cytokine storm [5–8]. Hypoxia status, neutrophil count, and cytokine storm all reflect the degree of lung oxidative stress and disease severity. Oxidative stress could induce dose dependent lung tissue injury ranging from apoptosis to necrosis [45]. Respiratory burst is mediated by activated macrophages and neutrophils and generates reactive oxygen species including superoxide, hydrogen peroxide, and hydroxyl radicals [46]. SARS-COV-2 viral entry and replication in the lung tissue activates the viscous cycle starting with phagocyte mediated burst of reactive oxygen species and inflammatory cytokines that eventually triggers further tissue injury, cytokine release, activation of macrophages and neutrophils. Minor perturbation in oxidative balance could aid in controlling viral infection by causing measurable non-specific lethal effect to both infected host tissue and the viral pathogens [47]. However, delayed viral clearance as in the case of severe COVID-19 could results in depletion of cellular antioxidant resources, increase of reactive oxygen species products, and cytokine storm. Long term oxidative stress causes tissue damage through interaction between these free radicals and cellular lipids, proteins and DNA content [48].

Here we observed an overall dysregulation of oxidative stress genes expression in circulating blood and lung tissue during severe COVID-19 disease. MPO and S100A8/9 calprotectin's were the top upregulated oxidative markers in lung autopsies, whole blood, leucocytes, BALF derived macrophages and PBMC derived neutrophils. The three top upregulated oxidative genes were validated in blood of severe COVID-19 patients using qRT-PCR. Relative to uninfected donor controls, MPO, S100A8 and S100A9 were significantly higher in blood of severe versus asymptomatic COVID-19 patients. Interestingly, these three oxidative genes were also significantly upregulated in saliva of severe relative to asymptomatic COVID-19 patients (Fig. 4). This suggest that the saliva level of these oxidative genes can be used as non-invasive markers for COVID-19 disease severity.

S100A8 and S100A9 genes encode calcium binding proteins also known as Migration Inhibitory Factor-Related Protein 8 and 14 (MPR8 and MRP14), respectively. They form heterodimers known as calprotectin that binds to toll-like receptor 4 (TLR4) and function as alarmin to stimulate the innate immune system pathways, namely MAP-kinase and NF-kappa-B signaling [49,50]. Given that, S100A8 and S100A9 have extensive effects on the net inflammation, redox balance, and cell death via autophagy and apoptosis [51,52]. They are also expressed abundantly in cells of myeloid origin such as neutrophils and monocytes. These genes are not expressed in normal tissue resident macrophages, however, S100A9 (MRP14) was found to be expressed in macrophage during acute inflammation, while macrophage infiltrate during chronic inflammation expressed both S100A9 and S100A8 [53]. Interestingly, we found both S100A8 and S100A9 to be upregulated in BALF derived macrophages of severe COVID-19 in contrast to mild COVID-19 (Fig. 3A). Recently, Silvin et al. showed that elevated calprotectin levels in peripheral blood cells could be used to discriminate severe from mild COVID-19 infection [54]. In this study, they used high-dimensional flow cytometry and single-cell RNA sequencing of COVID-19 peripheral blood and suggested that high calprotectin production is mediated by abnormal myeloid subsets [54]. Calprotectin genes are also expressed in lungs, particularly in lung epithelial and alveolar type II pneumocytes [55]. Likewise, the expression of these genes is increased with viral infection [56] and lipopolysaccharide stimulation [57]. In our study, through bioinformatic analyses, we showed that S100A8 and S100A9 were expressed in NHBE and lung autopsies, and their expression was upregulated post SARS-COV-2 infection (Fig. 1D). The observed increase of these markers, especially in lung autopsies, could be attributed to the increase in expression of these genes in both inflammatory as well as structural lung cells. We then associated elevated calprotectin level to

severe COVID-19 (Fig. 2, Supplementary Fig. 1, Supplementary Fig. 2, Fig. 3 and Supplementary Table 2) and validated this in whole blood and saliva of COVID-19 patients (Fig. 4).

In both blood and lung autopsies, myeloperoxidase enzyme gene, MPO, was among the top three oxidative stress genes. This gene is mainly expressed in neutrophil, and it mediates catalysis of reactive oxygen intermediates such as hypohalous acids [58]. Oxidative stress stimulates neutrophil extracellular traps (NETs) formation by neutrophils, NETosis, and lead to burst of neutrophil granules containing myeloperoxidase enzyme and calprotectin which in turn boost the cellular oxidative levels further. Similar to S100A8 and S100A9, myeloperoxidase expression level was associated with disease severity (Fig. 2). Supporting these findings, a recent investigation by FP Veras et al. showed viable SARS-COV-2 ability to directly induce the release of NETs by healthy neutrophils [2]. This group observed that NETs concentration was increased in plasma, tracheal aspirate and lung autopsies during SARS-COV-2 infection. Other groups also reported association between MPO levels and COVID-19 severity [3,4].

Similar to other viral infections, it is difficult to differentiate between association and causation effects of SARS-COV-2 infection on oxidative stress mediated cellular injury [59]. Viral induced hypoxemia requires increasing the levels of inspired concentration of oxygen to maintain the systemic oxygen delivery [60]. A level of lung oxidative stress could then be induced corresponding to this increase in the level of inspired oxygen [60]. This may contribute to the observed increase in oxidative stress gene markers. More studies could be needed to determine the level of contribution of this potential source of oxidative stress. Recent findings suggest that SARS-COV-2 could directly promote neutrophil activation and release of NETs [61]. Through analysis of different respiratory infections, we have showed a prominent upregulation in oxidative stress genes during coronavirus infection (Fig. 5A) relative to other respiratory infections such as IAV and RSV infections. Recently, using rhesus macaques and mice infected with different viral infections, Guo et al. showed that the increase in S100A8 gene expression during COVID-19 infection is associated with disease severity; and suggest that it could contribute to the evasion mechanism induced by coronavirus infection [56]. Our bioinformatics analysis confirmed Guo et al. animal findings within human blood samples. Further, we have shown that beside S100A8, coronavirus infection also induced the increase of additional 26 oxidative related genes hinting at higher potential oxidative stress load in these infections.

The other noticeable dysregulated oxidative genes in our study were Sulfiredoxin-1 (SRXN1), Glutamate-cysteine ligase modifier (GCLM), and two antioxidant genes: Sestrin 2 (SESN2) and Thioredoxin (TXN). Respiratory virus induced oxidative stress is attributed to the increased expression of these genes in both lung inflammatory and structural cells. Different respiratory viral infections including influenza H5N1, RSV and coronavirus infections induce oxidative stress imbalance [24,62,63]. Lung injury and infection severity in these viral infections are directly related to the viral load, net inflammation, and level of oxidative stress [63]. Interestingly, viral induced lung injury could be attenuated by administration of exogenous antioxidants [62,64,65]. TXN with potent antioxidant properties was found to be elevated in alveolar macrophages and type II epithelial cells in the lungs of acute respiratory distress syndrome [66]. Whilst exogenous administration of thioredoxin decreased Influenza A Virus (H1N1)-Induced acute lung injury and inflammation in the lungs of the virus-infected mice [65,67]. More information is needed to better understand the role of oxidative markers such as SRXN1 in COVID-19 pathogenesis.

Targeting one or more of these oxidative stress gene could represent an effective therapeutic approach for the treatment of COVID-19 disease. This may hence prevent the progression of the disease to cytokine storm, coagulopathy, and extensive lung tissue necrosis. In fact, a recent animal study has showed that targeting calprotectin with administration of paquinimod reduced the neutrophil derived oxidative damage and helped in boosting host antiviral response [56]. SARS-COV-2 induced NRF2 suppression was also reversed through administration of NRF2 agonists, 4-OI and DMF [24]. Direct antioxidant such as Vitamin C are small molecules with short half-life, while NRF2 agonist deploy long lasting antioxidant effect by activating enzymatic reactions that persist days after elimination of this agonist [68,69].

Other selective antioxidant targeting myeloperoxidase could help in clearance of NETs, while macrophage ability to clear NETs could be enhanced by AMP-activated protein kinase (AMPK) activator such as Metformin or application of neutralizing antibody against HMGB1 [70].

In conclusion, SARS-COV-2 induce the expression of oxidative stress genes via both immune as well as lung structural cells. Myeloperoxidase and calprotectin gene levels are increased in blood, lung tissue, and inflammatory cells. In our study, these genes were detected in salivary samples and hence they could potentially be used as a non-invasive severe COVID-19 marker. The observed correlation between oxidative stress genes dysregulation and COVID-19 disease severity deserve more attention. These changes in oxidative stress gene expression may or may not reflect alteration in the net oxidative stress balance. It is warranted that further mechanistical studies are performed to confirm this association.

Declaration of competing interest

The authors declare no competing interests.

Acknowledgments

This research has been financially supported by Tissue Injury and Repair (TIR) group operational grant (Grant code: 150317); COVID-19 research grant (CoV19-0307), Seed grant (Grant code: 2001090275); and by collaborative research grant (Grant code: 2001090278) to RH, University of Sharjah, UAE; and by a Sandooq Al Watan Applied Research & Development grant to RH (SWARD-S20-007), UAE; and by Al Jalila Foundation Seed Grant (AJF202019), UAE; and by Prince Abdullah Ben Khalid Celiac Disease Research Chair, under the Vice Deanship of Research Chairs, King Saud University, Riyadh, Kingdom of Saudi Arabia.

Appendix A. Supplementary data

Supplementary data to this article can be found online at https://doi.org/10.1016/j.freeradbiomed.2021.06.018.

References

[1] H. Chen, J. Guo, C. Wang, F. Luo, X. Yu, W. Zhang, et al., Clinical characteristics and intrauterine vertical transmission potential of COVID-19 infection in nine pregnant women: a retrospective review of medical records, Lancet 395 (10226) (2020) 809–815.
[2] C. Huang, Y. Wang, X. Li, L. Ren, J. Zhao, Y. Hu, et al., Clinical features of patients infected with 2019 novel coronavirus in Wuhan, China, Lancet 395 (10223) (2020) 497–506.
[3] C. Rothe, M. Schunk, P. Sothmann, G. Bretzel, G. Froeschl, C. Wallrauch, et al., Transmission of 2019-nCoV infection from an asymptomatic contact in Germany, N. Engl. J. Med. 382 (10) (2020) 970–971.
[4] M.L. Holshue, C. DeBolt, S. Lindquist, K.H. Lofy, J. Wiesman, H. Bruce, et al., First case of 2019 novel coronavirus in the United States, N. Engl. J. Med. 382 (10) (2020) 929–936.
[5] S.A. Vardhana, J.D. Wolchok, The many faces of the anti-COVID immune response, J. Exp. Med. 217 (6) (2020).
[6] D. Blanco-Melo, B.E. Nilsson-Payant, W.-C. Liu, S. Uhl, D. Hoagland, R. Møller, et al., Imbalanced host response to SARS-CoV-2 drives development of COVID-19, Cell 181 (5) (2020) 1036–1045, e9.
[7] J.S. Lee, S. Park, H.W. Jeong, J.Y. Ahn, S.J. Choi, H. Lee, et al., Immunophenotyping of COVID-19 and influenza highlights the role of type I interferons in development of severe COVID-19, Science Immunology 5 (49) (2020), eabd1554.
[8] M. Liao, Y. Liu, J. Yuan, Y. Wen, G. Xu, J. Zhao, et al., Single-cell landscape of bronchoalveolar immune cells in patients with COVID-19, Nat. Med. 26 (6) (2020) 842–844.
[9] A.K. Singh, C.L. Gillies, R. Singh, A. Singh, Y. Chudasama, B. Coles, et al., Prevalence of co-morbidities and their association with mortality in patients with

COVID-19: a systematic review and meta-analysis, Diabetes Obes. Metabol. 22 (10) (2020) 1915–1924.
[10] N. Stefan, A.L. Birkenfeld, M.B. Schulze, Global pandemics interconnected — obesity, impaired metabolic health and COVID-19, Nat. Rev. Endocrinol. 17 (3) (2021) 135–149.
[11] L.Y.W. Lee, J.-B. Cazier, T. Starkey, S.E.W. Briggs, R. Arnold, V. Bisht, et al., COVID-19 prevalence and mortality in patients with cancer and the effect of primary tumour subtype and patient demographics: a prospective cohort study, Lancet Oncol. 21 (10) (2020) 1309–1316.
[12] A.R. Hofstetter, J.A. De La Cruz, W. Cao, J. Patel, J.A. Belser, J. McCoy, et al., NADPH oxidase 1 is associated with altered host survival and T cell phenotypes after influenza A virus infection in mice, PloS One 11 (2) (2016) e0149864-e.
[13] L. Zhu, L. Liu, Y. Zhang, L. Pu, J. Liu, X. Li, et al., High level of neutrophil extracellular traps correlates with poor prognosis of severe influenza A infection, J. Infect. Dis. 217 (3) (2018) 428–437.
[14] Y.M. Hosakote, P.D. Jantzi, D.L. Esham, H. Spratt, A. Kurosky, A. Casola, et al., Viral-mediated inhibition of antioxidant enzymes contributes to the pathogenesis of severe respiratory syncytial virus bronchiolitis, Am. J. Respir. Crit. Care Med. 183 (11) (2011) 1550–1560.
[15] I. Hamming, W. Timens, M.L.C. Bulthuis, A.T. Lely, G.J. Navis, H. van Goor, Tissue distribution of ACE2 protein, the functional receptor for SARS coronavirus. A first step in understanding SARS pathogenesis, J. Pathol. 203 (2) (2004) 631–637.
[16] I.T. Lee, T. Nakayama, C.-T. Wu, Y. Goltsev, S. Jiang, P.A. Gall, et al., ACE2 localizes to the respiratory cilia and is not increased by ACE inhibitors or ARBs, Nat. Commun. 11 (1) (2020) 5453.
[17] S. Haga, N. Yamamoto, C. Nakai-Murakami, Y. Osawa, K. Tokunaga, T. Sata, et al., Modulation of TNF-α-converting enzyme by the spike protein of SARS-CoV and ACE2 induces TNF-α production and facilitates viral entry, Proc. Natl. Acad. Sci. Unit. States Am. 105 (22) (2008) 7809–7814.
[18] M Hoffmann, H Kleine-Weber, S Schroeder, N Krüger, T Herrler, S Erichsen, et al SARS-CoV-2 cell entry depends on ACE2 and TMPRSS2 and is blocked by a clinically proven protease inhibitor, Cell 181 (2) (2020) 271–280.e278.
[19] C. Vickers, P. Hales, V. Kaushik, L. Dick, J. Gavin, J. Tang, et al., Hydrolysis of biological peptides by human angiotensin-converting enzyme-related carboxypeptidase *, J. Biol. Chem. 277 (17) (2002) 14838–14843.
[20] P. Verdecchia, C. Cavallini, A. Spanevello, F. Angeli, The pivotal link between ACE2 deficiency and SARS-CoV-2 infection, Eur. J. Intern. Med. 76 (2020) 14–20.
[21] I.G. Fernandes, C.A. de Brito, V.M.S. dos Reis, M.N. Sato, N.Z. Pereira, SARS-CoV-2 and other respiratory viruses: what does oxidative stress have to do with it? Oxidative Medicine and Cellular Longevity 2020 (2020), 8844280.
[22] J.W. Kaspar, S.K. Niture, A.K. Jaiswal, Nrf2:INrf2 (Keap1) signaling in oxidative stress, Free Radic. Biol. Med. 47 (9) (2009) 1304–1309.
[23] S.K. Niture, R. Khatri, A.K. Jaiswal, Regulation of Nrf2—an update, Free Radic. Biol. Med. 66 (2014) 36–44.
[24] D. Olagnier, E. Farahani, J. Thyrsted, J. Blay-Cadanet, A. Herengt, M. Idorn, et al., SARS-CoV2-mediated suppression of NRF2-signaling reveals potent antiviral and anti-inflammatory activity of 4-octyl-itaconate and dimethyl fumarate, Nat. Commun. 11 (1) (2020) 4938.
[25] A.K. Kalem, B. Kayaaslan, S. Neselioglu, F. Eser, İ. Hasanoglu, A. Aypak, et al., A useful and sensitive marker in the prediction of COVID-19 and disease severity: Thiol, Free Radic. Biol. Med. 166 (2021) 11–17.
[26] D. Singh, H. Wasan, K.H. Reeta, Heme oxygenase-1 modulation: a potential therapeutic target for COVID-19 and associated complications, Free Radic. Biol. Med. 161 (2020) 263–271.
[27] I.H.K. Reyes, A. Pico, Rashid K. Wikipathways, Oxidative stress (Homo sapiens), Available at: www.wikipathways.org/index.php/Pathway:WP408, 2016. (Accessed 2 December 2020).
[28] Y. Morel, R. Barouki, Repression of gene expression by oxidative stress, Biochem. J. 342 Pt 3 (Pt 3) (1999) 481–496.
[29] Y.-M. Go, J.D. Chandler, D.P. Jones, The cysteine proteome, Free Radic. Biol. Med. 84 (2015) 227–245.
[30] T.S. Hoskin, J.M. Crowther, J. Cheung, M.J. Epton, P.D. Sly, P.A. Elder, et al., Oxidative cross-linking of calprotectin occurs in vivo, altering its structure and susceptibility to proteolysis, Redox Biology 24 (2019), 101202.
[31] J.L. Martindale, N.J. Holbrook, Cellular response to oxidative stress: signaling for suicide and survival*, J. Cell. Physiol. 192 (1) (2002) 1–15.
[32] M. Wu, Y. Chen, H. Xia, C. Wang, C.Y. Tan, X. Cai, et al., Transcriptional and proteomic insights into the host response in fatal COVID-19 cases, Proc. Natl. Acad. Sci. Unit. States Am. 117 (45) (2020) 28336.
[33] A.C. Aschenbrenner, M. Mouktaroudi, B. Kraemer, N. Antonakos, M. Oestreich, K. Gkizeli, et al., Disease Severity-specific Neutrophil Signatures in Blood Transcriptomes Stratify COVID-19 Patients. medRxiv, 2020, 2020.07.07.20148395.
[34] K.A. Overmyer, E. Shishkova, I.J. Miller, J. Balnis, M.N. Bernstein, T.M. Peters-Clarke, et al., Large-scale multi-omic analysis of COVID-19 severity, Cell Syst (2020).
[35] M.E. Charlson, P. Pompei, K.L. Ales, C.R. MacKenzie, A new method of classifying prognostic comorbidity in longitudinal studies: development and validation, J. Chron. Dis. 40 (5) (1987) 373–383.
[36] M.E. Ritchie, B. Phipson, D.I. Wu, Y. Hu, C.W. Law, W. Shi, et al., Limma powers differential expression analyses for RNA-sequencing and microarray studies, Nucleic Acids Res. 43 (7) (2015) e47–e.
[37] A.K. Zaas, M. Chen, J. Varkey, T. Veldman, A.O. Hero 3rd, J. Lucas, et al., Gene expression signatures diagnose influenza and other symptomatic respiratory viral infections in humans, Cell Host Microbe 6 (3) (2009) 207–217.
[38] R. Reghunathan, M. Jayapal, L.Y. Hsu, H.H. Chng, D. Tai, B.P. Leung, et al., Expression profile of immune response genes in patients with Severe Acute Respiratory Syndrome, BMC Immunol. 6 (2005) 2.
[39] J.J. Hughey, A.J. Butte, Robust meta-analysis of gene expression using the elastic net, Nucleic Acids Res. 43 (12) (2015) e79–e.
[40] A.J. Wilk, A. Rustagi, N.Q. Zhao, J. Roque, G.J. Martínez-Colón, J.L. McKechnie, et al., A single-cell atlas of the peripheral immune response in patients with severe COVID-19, Nat. Med. 26 (7) (2020) 1070–1076.
[41] Available from: www.cdc.gov. (Accessed 9 September 2020) https://www.cdc.gov/coronavirus/2019-ncov/lab/guidelines-clinical-specimens.html.
[42] J.S. Muhammad, N. Saheb Sharif-Askari, Z.-G. Cui, M. Hamad, R. Halwani, SARS-CoV-2 infection-induced promoter hypomethylation as an epigenetic modulator of heat shock protein A1L (HSPA1L) gene, Front. Genet. 12 (129) (2021).
[43] S. Goel, F. Saheb Sharif-Askari, N. Saheb Sharif-Askari, B. Mdkhana, B. Mahboub, A.M. Zakri, et al., SARS-CoV-2 Switches 'on' MAPK and NF_k B signaling via the reduction of nuclear DUSP1 and DUSP5 expression, Front. Pharmacol. 12 (2021) 404.
[44] S.V. Kuchipudi, M. Tellabati, R.K. Nelli, G.A. White, B.B. Perez, S. Sebastian, et al., 18S rRNA is a reliable normalisation gene for real time PCR based on influenza virus infected cells, Virol. J. 9 (1) (2012) 1–7.
[45] S.V. Lennon, S.J. Martin, T.G. Cotter, Dose-dependent induction of apoptosis in human tumour cell lines by widely diverging stimuli, Cell Prolif 24 (2) (1991) 203–214.
[46] F.C. Camini, C.C. da Silva Caetano, L.T. Almeida, C.L. de Brito Magalhães, Implications of oxidative stress on viral pathogenesis, Arch. Virol. 162 (4) (2017) 907–917.
[47] C. Nathan, M.U. Shiloh, Reactive oxygen and nitrogen intermediates in the relationship between mammalian hosts and microbial pathogens, Proc. Natl. Acad. Sci. U. S. A. 97 (16) (2000) 8841–8848.
[48] G. Pizzino, N. Irrera, M. Cucinotta, G. Pallio, F. Mannino, V. Arcoraci, et al., Oxidative Stress: Harms and Benefits for Human Health. Oxidative Medicine and Cellular Longevity, 2017, 8416763, 2017.
[49] M. Riva, E. Källberg, P. Björk, D. Hancz, T. Vogl, J. Roth, et al., Induction of nuclear factor-κB responses by the S100A9 protein is Toll-like receptor-4-dependent, Immunology 137 (2) (2012) 172–182.
[50] J.C. Simard, D. Girard, P.A. Tessier, Induction of neutrophil degranulation by S100A9 via a MAPK-dependent mechanism, J. Leukoc. Biol. 87 (5) (2010) 905–914.
[51] S. Ghavami, M. Eshragi, S.R. Ande, W.J. Chazin, T. Klonisch, A.J. Halayko, et al., S100A8/A9 induces autophagy and apoptosis via ROS-mediated cross-talk between mitochondria and lysosomes that involves BNIP3, Cell Res. 20 (3) (2010) 314–331.
[52] C. Ryckman, K. Vandal, P. Rouleau, M. Talbot, P.A. Tessier, Proinflammatory activities of S100: proteins S100A8, S100A9, and S100A8/A9 induce neutrophil chemotaxis and adhesion, J. Immunol. 170 (6) (2003) 3233–3242.
[53] K. Odink, N. Cerletti, J. Brüggen, R.G. Clerc, L. Tarcsay, G. Zwadlo, et al., Two calcium-binding proteins in infiltrate macrophages of rheumatoid arthritis, Nature 330 (6143) (1987) 80–82.
[54] A. Silvin, N. Chapuis, G. Dunsmore, A.G. Goubet, A. Dubuisson, L. Derosa, et al., Elevated calprotectin and abnormal myeloid cell subsets discriminate severe from mild COVID-19, Cell 182 (6) (2020) 1401–1418, e18.
[55] O.S. Kotsiou, D. Papagiannis, R. Papadopoulou, K.I. Gourgoulianis, Calprotectin in lung diseases, Int. J. Mol. Sci. 22 (4) (2021) 1706.
[56] Q. Guo, Y. Zhao, J. Li, J. Liu, X. Yang, X. Guo, et al., Induction of alarmin S100A8/A9 mediates activation of aberrant neutrophils in the pathogenesis of COVID-19, Cell Host Microbe 29 (2) (2021) 222–235, e4.
[57] M.O. Henke, A. Renner, B.K. Rubin, J.I. Gyves, E. Lorenz, J.S. Koo, Up-regulation of S100A8 and S100A9 protein in bronchial epithelial cells by lipopolysaccharide, Exp. Lung Res. 32 (8) (2006) 331–347.
[58] Y. Aratani, Myeloperoxidase: its role for host defense, inflammation, and neutrophil function, Arch. Biochem. Biophys. 640 (2018) 47–52.
[59] K.B. Schwarz, Oxidative stress during viral infection: a review, Free Radic. Biol. Med. 21 (5) (1996) 641–649.
[60] M. Nakane, Biological effects of the oxygen molecule in critically ill patients, Journal of Intensive Care 8 (1) (2020) 95.
[61] F.P. Veras, M.C. Pontelli, C.M. Silva, J.E. Toller-Kawahisa, M. de Lima, D. C. Nascimento, et al., SARS-CoV-2-triggered neutrophil extracellular traps mediate COVID-19 pathology, J. Exp. Med. 217 (12) (2020), e20201129.
[62] S.-H. Huang, X.-J. Cao, W. Liu, X.-Y. Shi, W. Wei, Inhibitory effect of melatonin on lung oxidative stress induced by respiratory syncytial virus infection in mice, J. Pineal Res. 48 (2) (2010) 109–116.
[63] G. He, C. Dong, Z. Luan, B.M. McAllan, T. Xu, L. Zhao, et al., Oxygen free radical involvement in acute lung injury induced by H5N1 virus in mice, Influenza and Other Respiratory Viruses 7 (6) (2013) 945–953.
[64] J.A. Espinoza, P.A. González, A.M. Kalergis, Modulation of antiviral immunity by heme oxygenase-1, Am. J. Pathol. 187 (3) (2017) 487–493.
[65] R. Tanaka, Y. Ishima, Y. Enoki, K. Kimachi, T. Shirai, H. Watanabe, et al., Therapeutic impact of human serum albumin–thioredoxin fusion protein on influenza virus-induced lung injury mice, Front. Immunol. 5 (561) (2014).
[66] M.E. Callister, A. Burke-Gaffney, G.J. Quinlan, A.G. Nicholson, R. Florio, H. Nakamura, et al., Extracellular thioredoxin levels are increased in patients with acute lung injury, Thorax 61 (6) (2006) 521–527.
[67] M. Yashiro, H. Tsukahara, A. Matsukawa, M. Yamada, Y. Fujii, Y. Nagaoka, et al., Redox-active protein thioredoxin-1 administration ameliorates influenza A virus (H1N1)-induced acute lung injury in mice, Crit. Care Med. 41 (1) (2013).

[68] A. Cuadrado, M. Pajares, C. Benito, J. Jiménez-Villegas, M. Escoll, R. Fernández-Ginés, et al., Can activation of NRF2 Be a strategy against COVID-19? Trends Pharmacol. Sci. 41 (9) (2020) 598–610.
[69] A.T. Dinkova-Kostova, P. Talalay, Direct and indirect antioxidant properties of inducers of cytoprotective proteins, Mol. Nutr. Food Res. 52 (Suppl 1) (2008) S128–S138.
[70] M. Grégoire, F. Uhel, M. Lesouhaitier, A. Gacouin, M. Guirriec, F. Mourcin, et al., Impaired efferocytosis and neutrophil extracellular trap clearance by macrophages in ARDS, Eur. Respir. J. 52 (2) (2018), 1702590.